



Evaluation of Code-Based Long-Term Deflection of Prestressed Concrete Beam

Sholihah, E.A., Kristiawan, S.A., and Saifullah, H.A.

Department of Civil Engineering, Sebelas Maret University, Surakarta, Indonesia

Received: 08/01/2025

Revised: 07/04/2025

Accepted: 15/04/2025

ABSTRACT: Long-term deflection in prestressed concrete is influenced by several factors, including shrinkage, creep, and the relaxation of the prestressing steel. While these factors are crucial for the serviceability of prestressed beams, concrete design codes often quantify their effects using simplified methods. This simplification raises concerns about the accuracy of long-term predictions. This paper evaluates the code-based long-term deflection of prestressed concrete beams and compares the results with the displacement method, which is regarded as a more accurate alternative for estimating the effect of shrinkage, creep, and relaxation on long-term deflection. A sensitivity analysis was also conducted to determine the sensitivity of parameters to affect the long-term deflection. The results indicate that code-based methods (ACI 209R-92 and FIB 2010) give a lower estimation (within 4%) of deflection compared to the displacement method. This seemingly minor deviation may raise serious concerns in circumstances where tolerances are strict or structural integrity is critical. The sensitivity analysis identifies relative humidity as the most significant parameter affecting deflection. The outcome of this detailed study paved the way to properly select and utilize shrinkage and creep models, taking into consideration the key contributing factors affecting the long-term deflection.

Keywords: shrinkage, creep, relaxation, long-term deflection, prestressed beam

1. Introduction

In the design of reinforced concrete buildings, the susceptibility of concrete elements to cracking, attributed to the material's low tensile strength, can be mitigated by providing adequate reinforcements. Other design parameters, such as the deflection limits, are typically addressed by adjusting the dimension of the reinforced concrete elements. The application of reinforced concrete in long-span beams presents challenges due to significant internal stresses and deflections (Kristiawan and Nugroho, 2017). To address these issues, prestressing forces are introduced to reduce tensile stresses in the concrete, thereby minimizing cracking and excessive deflection (Gilbert, 2001).

A literature review on the deflection of reinforced concrete beams identifies key variables affecting deflection behavior, categorized into structural and material factors. Structural factors include the reinforcement ratio (Peng *et al.*, 2025), reinforcement lap splice (El-Azab and Mohamed, 2014), and tension stiffening (Teng *et al.*, 2022). Other researcher noted that a modification of shear reinforcement can also improve the flexural capacity and ductility (Bello *et al.*, 2024; Ghoniem *et al.*, 2024). On the material side, the mechanical characteristics of concrete and steel significantly influence the RC beam's deflection. For example, utilizing high-strength steel reinforced ultra-high-performance concrete (HSSRUHPC) yields a different short-term flexural stiffness calculation method to account for the constraining effect of high-strength steel sections on ultra-high performance concrete (UHPC) and the tensile properties of UHPC (Peng *et al.*, 2025). Meanwhile, creep and shrinkage are the relevant material properties that influence deflection in the long term (Fang *et al.*, 2021).

A significant challenge in the long-term performance of prestressed beams is the loss of prestress, primarily due to concrete shrinkage, creep, and steel relaxation. These phenomena can alter the stress–strain relationship and deflection of the beams, potentially compromising serviceability (Han *et al.*, 2023a; Zhang *et al.*, 2023). While concrete design codes provide guidelines for accounting for shrinkage and creep effects, the simplified calculations prescribed in these codes may not consistently yield optimal design solutions.

Utilizing codes as a reference for predicting creep and shrinkage aids engineers in estimating their impact on long-term deflection. These deflection estimations enable designers to assess whether the design of reinforced concrete or prestressed concrete beam elements conform to serviceability requirements. Codes developed by the American Association of State Highway and Transportation Officials (AASHTO), the American Concrete Institute (ACI), the European Committee for Standardization, the Fédération Internationale du Béton (fib), and the Comité Européen du Béton (CEB) are widely recognized and implemented across continents. Several countries have adopted these codes, modifying them to align with their regulatory frameworks. For instance, Indonesia has integrated the ACI standards into its National Standard for concrete structures. This adaptation helps local construction engineers and practitioners stay aligned with cutting-edge developments in global best practices and ensures that national standards maintain coherence with internationally accepted methodologies. Based on the study by Shurbert-Hetzel *et al.*, 2023, the uncalibrated ACI model exhibited significantly better performance than the other five models evaluated. This enhanced effectiveness can be attributed to the comprehensive array of parameters utilized (10 input variables) and the inclusion of the integrated tuning time-ratio constant inherent to the ACI 209 model. However,

all the uncalibrated prediction models for creep and shrinkage still produce large deviations, so calibrated models are needed to improve the predictions (Shurbert-Hetzel *et al.*, 2023).

One crucial aspect to consider when selecting models for predicting shrinkage and creep is, in addition to their accuracy, their simplicity. The ACI 209R-08 model emerged as a good option. Even though it requires multiple inputs, it involves a few simple calculation steps. As a result, the ACI 209R-08 model may be the first choice for conducting shrinkage and creep analyses in practical applications. The CEB-FIP 1990 model shares the same inputs related to environmental factors as the ACI 209 model but varies in the extent and detail of the concrete mix factors it considers. Hence, CEB-FIP 1990 can be a good alternative for comparison purposes.

Once the effects of creep and shrinkage are determined, their impact on the long-term deflection of reinforced or prestressed concrete beams can be evaluated using code-based methods such as the ACI 209R-92 approach or the FIB 2010 model, among others. Each method possesses unique characteristics relevant to the behavioral analysis of concrete structures. The ACI 209R-92 provides a clear and empirically validated framework, making it suitable for a wide range of applications. However, the dependency on the linearity can constrain its precision when assessing structures characterized by complex geometries and a significant intensity of cracks. The FIB 2010 model adopts a more advanced approach, incorporating factors such as temperature and concrete age, which enables more precise calculations under challenging conditions. Nevertheless, this increased accuracy comes with added complexity; it requires more data and may present greater challenges in implementation compared to the ACI 209R-92. Meanwhile, the non-code-based displacement method excels in analyzing structural displacements and deformations, successfully accommodating complex behaviors such as those caused by dynamic loads. However, its technical intricacies and need for detailed assumptions and datasets can complicate its application, particularly in larger projects or when information is limited. As such, selecting the appropriate method depends on the project's specific requirements and the desired accuracy level. ACI 209R-92 is a pragmatic choice for simpler scenarios or static analyses due to its user-friendly nature. In contrast, for projects that demand greater precision and need to account for extreme environmental conditions, the FIB 2010 model is more suitable. While the displacement method is complex, it is invaluable for analyzing structures subject to significant variations or dynamic influences. Ultimately, engineers should align their method selection with the project's complexity, data availability, and accuracy requirements in concrete structure design.

This study aimed to evaluate the long-term deflection of prestressed beams caused by shrinkage, creep, and steel relaxation, as defined by two design codes. The analysis began with an examination of the shrinkage, creep, and relaxation properties of prestressed concrete materials, based on ACI 209R-08 and CEB-FIP 1990. The creep and shrinkage estimated by these two models were subsequently applied to estimate long-term deflection using simplified code-based models, specially ACI 209R-92 and FIB 2010. An alternative approach employing the displacement method was proposed to assess the accuracy of the code-based deflection (Reybrouck *et al.*, 2020). Furthermore, this current study will provide more benefits by analyzing the sensitivity of long-term deflection to factors affecting shrinkage, creep, and relaxation in prestressed beams (Cui and Wu, 2024; Yang *et al.*, 2020). The findings of this study provide a valuable reference for evaluating the design efficiency of prestressed beams with respect to their long-term deflection performance (Aili and Torrenti, 2020; Zhang and Hamed, 2020; Zhou *et al.*, 2022; Zhu *et al.*, 2020).

2. Shrinkage, Creep, and Relaxation Models

Concrete shrinkage occurs due to the evaporation of internal water, driven by the humidity gradient between the wet concrete and its surrounding environment. This process begins after the concrete has cured, with shrinkage occurring rapidly during the initial stages of drying and gradually slowing as the drying process progresses. Shrinkage leads to a reduction in concrete dimensions, which consequently diminishes the prestressing force. Another time-dependent deformation observed in concrete is creep, characterized by the gradual deformation of the material under sustained stress. This phenomenon arises from the viscoelastic properties of concrete, which cause it to gradually deform and shorten under constant stress. Creep results in a reduction of the prestressing force and an increase in the deflection of the structure over time. Various concrete design codes, including ACI 209R-08 and CEB-FIP 1990, offer models to estimate the behavior of creep and shrinkage in concrete.

2.1. ACI 209R-08 Model

ACI 209R-92 defines notional coefficients to estimate the creep and shrinkage behaviors of concrete based on its material properties and environmental factors. The model takes into account several factors, including relative humidity, surface-to-volume ratio, slump, fine aggregate content, cement content, air content, and the initial moisture curing conditions, when estimating shrinkage strain. The simplified calculation for shrinkage characteristics can be derived from the formula presented in Eqs. (1).

$$(\varepsilon_{sh})_t = \frac{t}{35+t} (\varepsilon_{sh})_u \quad (1)$$

where t is the age of concrete in days and $(\varepsilon_{sh})_u$ is the ultimate shrinkage.

The creep coefficient is influenced by factors such as the age at the time of loading, environmental relative humidity, member size, slump, fine aggregate content, and air content. The simplified calculation for creep characteristics can be derived from the following equation.

$$\phi_t = \frac{t^{0.60}}{10+t^{0.60}} \phi_u \quad (2)$$

where, t is the age of the concrete in days and ϕ_u is the ultimate creep.

2.2. CEB-FIP 1990 Model

The shrinkage and creep models based on CEB-FIP 1990 were developed from extensive empirical research and testing. The model takes into account factors such as concrete age, drying time, relative humidity, volume-to-surface ratio, cement type, and compressive strength to estimate shrinkage strain. The shrinkage model is presented in Eqs. (2).

$$(\varepsilon_{cs})_t = \varepsilon_{cs0} \beta_s (t - t_s) \quad (3)$$

where ε_{cs0} is the notional shrinkage coefficient, β_s is the coefficient that describes the development of shrinkage with time, t is the age of concrete in days, and t_s is the age of concrete (days) at the beginning of shrinkage.

The creep coefficient is predicted by considering factors such as concrete age, time of loading, relative humidity, volume-to-surface ratio, cement type, and compressive strength. The model for predicting the creep coefficient is given by

$$\phi_t = \phi_0 \beta_c (t - t_0) \quad (4)$$

where ϕ_0 is the notional creep coefficient and β_c is the coefficient that describes the development of creep with time after loading.

2.3. Steel Relaxation

Steel relaxation in prestressed concrete occurs as a result of sustained tensile force, leading to a loss of prestress over time. This relaxation process is evaluated by considering both short- and long-term relaxation losses. The formula for calculating steel relaxation in prestressed concrete is derived from a combination of empirical methods and theoretical analysis. Additionally, factors such as temperature and humidity are considered in the calculation of steel relaxation, which may require adjustments to the formulas to account for specific conditions in prestressed concrete. Furthermore, a reduction coefficient is applied to modify the stress loss values based on the ratio of the initial stress to the yield strength of the steel. This approach enables the adaptation of the formula to accommodate various types of prestressing steels with different material characteristics.

Using this method, the steel relaxation formula can be incorporated to predict the loss of prestressing force, which aids in the safety and serviceability design of prestressed concrete structures. The simplified calculation for steel relaxation can be performed using Eqs. (3).

$$\frac{\Delta\sigma_{pr}}{\sigma_{p0}} = -\frac{\log(\tau - t_0)}{45} \left(\frac{\sigma_{p0}}{f_{py}} - 0.55 \right) \quad (5)$$

where τ represents the time since prestressing was applied, t_0 is the initial time at which prestressing was applied, σ_{p0} is the tendon tensile stress due to prestress, and f_{py} is the yield stress of the steel.

3. Long-term deflection

Code-based deflection formulas are simplified methods that integrate the fundamental principles of structural mechanics with simplified analytical techniques. Beam stiffness plays a critical role in determining the extent of deflection under applied loads. By calculating the stiffness using the modulus of elasticity and moment of inertia of the cross-section, the deflection of a beam can be estimated using these code-based formulas. ACI 209R-92 and FIB 2010 are examples of code-based deflection methods that will be evaluated in this study. Both methods rely on a set of assumptions and simplifications to provide straightforward procedures for calculating deflection more rapidly. However, this approach may reduce accuracy, particularly when addressing the complexities of long-term phenomena such as shrinkage and creep.

More precise deflection calculations can be achieved using the displacement method. This method derives the deflection formula through an analytical approach that integrates the principles of structural mechanics and elasticity theory. It adheres to the fundamental principles

of equilibrium, displacement relationships, and the deformation compatibility to establish a system of equations. By employing this approach, the deflection formula provides a more accurate estimation of the structural deformation. The accuracy of the displacement method has been confirmed by an agreement between the long-term estimated and experimental deflection (Reybrouck *et al.*, 2020).

3.1. Long-term Deflection Based on ACI 209R-92

In general, the deflections in prismatic members subjected to uniformly distributed loads can be computed using (ACI 209R-92, 1997) in Eqs. (4).

$$a_m = \frac{5\ell^2}{48EI} \left[M_m + \frac{1}{10}(M_A + M_B) \right] \quad (6)$$

where a_m is the deflection at midspan, ℓ is the span length, E is the modulus of elasticity, and I is the moment of inertia. The moments M_m , M_A , and M_B , correspond to the midspan and moments at the two ends, respectively. For general loading and boundary conditions, Eqs. (6) can be expressed as Eqs. (7) to estimate short-term deflections, $(a_i)_D$ due to dead loads at the onset of loading.

$$(a_i)_D = \xi M_D \ell^2 / E_{ci} I_e \quad (7)$$

where ξ is a deflection coefficient, M_D is the moment due to dead load, ℓ is the span length, E_{ci} is the modulus of elasticity of the concrete at the time of initial load, and I_e is the effective moment of inertia. The effective moment of the area is used in the equation to predict the occurrence of cracking in the beams due to the applied load. The short-term deflection represents the initial response of the beam under loading. Subsequently, additional long-term deflections resulting from creep are superimposed using Eqs. (5).

$$(a_t)_D = \xi_r v_t (a_i)_D \quad (8)$$

where ξ_r is reduction factor that accounts for the effects of compression steel, the movement of neutral axis, and progressive cracking in reinforced flexural members, and v_t refers to the creep coefficient at any given time. The deflection due to creep, as given in Eqs. (8), suggests that it is proportional to the initial dead-load deflection, $(a_i)_D$. Meanwhile, another time-dependent deflection resulting from shrinkage warping can be calculated using is Eqs. (6).

$$a_{sh} = \xi_w \phi_{sh} \ell^2 \quad (9)$$

where ξ_w is a deflection coefficient that accounts for boundary conditions, ϕ_{sh} is the curvature due to shrinkage warping, and ℓ is the span length. Finally, the deflection due to the live load can be calculated using Eqs. (7).

$$(a_i)_L = (a_i)_{D+L} - (a_i)_D \frac{E_{ci}}{E_c} \quad (10)$$

where $(a_i)_{D+L}$ is the initial deflection due to both dead and live loads, $(a_i)_D$ is the initial dead load deflection, and the ratio $\frac{E_{ci}}{E_c}$ represents the ratio of the elastic modulus of concrete at the time of initial loading to its elastic modulus at service loading. For a prestressed member, additional deflection should be considered, for example, the deflection caused by the prestressing cables. In the cable trajectory forms a parabola, the deflection can be calculated using Eqs. (8). It should be noted that the deflection due to the prestress force tends to cause the beam to bend upwards. To account for the loss of prestressing force, Eqs. (9) is used:

$$a_1 = \frac{5P_i e L^2}{48 EI} \quad (11)$$

$$\delta_{pi} = \left[-\frac{\Delta P}{P_i} + (K_r \cdot v_t) x \left(1 - \frac{\Delta P}{2P_i} \right) \right] a_1 \quad (12)$$

where a_1 is the deflection due to prestressing steel, P_i is the initial prestressing force, e is the eccentricity of the prestressing steel, E is the modulus of elasticity of the beam, L is the span length of the beam, I is the moment inertia of the beam, K_r represent a coefficient related to resistance or stiffness, v_t is creep coefficient, and ΔP is the change in prestress force at time t . Thus, in general, the total deflection of a prestressed concrete member at any time is given by Eqs. (10).

$$a_t = \overbrace{a_1 + \delta_{pi}}^{(1)} - \left[\overbrace{(a_i)_D}^{(2)} + \overbrace{(a_t)_D}^{(3)} + \overbrace{\hat{a}_{sh}}^{(4)} + \overbrace{(a_i)_L}^{(5)} \right] \quad (13)$$

where:

Term (1) represents the initial load deflection due to the prestressing, as given by Eqs. (11) and (12)

Term (2) represents the initial dead-load deflection, as given by Eqs. (7)

Term (3) represents the creep deflection due to dead-load, as given by Eqs. (8)

Term (4) represents the deflection due to shrinkage warping, as given by Eqs. (9)

Term (5) represents the live-load deflection, as given by Eqs. (10).

The ACI 209R-92 method offers a straightforward and practical approach for calculating long-term deflections in prestressed concrete beams; however, it has certain limitations that may hinder its performance in cases involving modern concrete mixtures, extreme environmental conditions, or complex loading histories. This method was developed based on data from normal-strength concrete, specifically up to 40 MPa. The method may either underestimate or overestimate long-term deflections for high-strength concrete or contemporary mixtures that include supplementary cementitious materials such as fly ash or silica fume. Additionally, it assumes standard environmental conditions, typically around 40% relative humidity and 20°C temperature. Predictive deflections may vary significantly from actual behavior under extreme conditions—such as very dry or humid climates. The method also fails to consider loading history, which is critical in variable or cyclic loading scenarios. Furthermore, it assumes that sections remain uncracked or only lightly cracked, which may lead to underestimating deflections in beams experiencing significant cracking, particularly under high service loads.

3.2. Long-term Deflection Based on Fib Model 2010

The Prediction of deflection according FIB 2010 Model is expressed in Eqs. (11).

$$a = \zeta a_{II} + (1 - \zeta)a_I \quad (14)$$

where a is the deflection, a_I, a_{II} are the deflection values calculated for the uncracked and fully cracked conditions respectively, and ζ is an interpolation coefficient (allowing for the effect of tension stiffening at a section) given by expression in Eqs. (12).

$$\zeta = 1 - \beta \left(\frac{\sigma_{sr}}{\sigma_s} \right)^2 \quad (15)$$

where β is a coefficient that accounts for the influence of the duration of loading or repeated loading on the average strain, σ_{sr} is the stress in the tension reinforcement calculated based on a cracked section under the loading conditions that cause first cracking, and σ_s represents the stresses in the tension reinforcement and is calculated based on a cracked section under the applied load. For loads with a sufficiently long duration to cause creep, the total deformation including creep, is calculated using the effective modulus of elasticity of concrete, as given in Eqs. (13).

$$E_{c,eff} = \frac{E_{cm}}{1 + \varphi} \quad (16)$$

where E_{cm} is modulus of elasticity for concrete and φ is the creep coefficient corresponding to the load and time interval. The deformation of a reinforced concrete beam due to a sustained load can be expressed in terms of the flexural curvature, as given by Eqs. (14).

$$\frac{1}{r_n} = \zeta \frac{M}{E_{c,eff} I_c} + (1 - \zeta) \frac{M}{E_{c,eff} I_u} \quad (17)$$

where M is the bending moment due to the applied load, $E_{c,eff}$ is the effective modulus of elasticity of concrete considering the long-term duration of the load (sustained load), ζ is an interpolation coefficient, I_c is the second moment of area for cracked condition, and I_u is the second moment of area for uncracked condition. The effect of shrinkage on curvature can be assessed using Eqs. (15).

$$\frac{1}{r_{cs}} = \varepsilon_{cs} \cdot \alpha_e \cdot \frac{S}{I} \quad (18)$$

where $1/r_{cs}$ is the curvature due to shrinkage, ε_{cs} is the free shrinkage strain, S is the first moment of the area of reinforcement about the centroid of the section, I is the second moment of the area of the section, and α_e is the effective modular ratio = $E_s/E_{c,eff}$. Hence, the total curvature due to the applied load, creep, and shrinkage can be calculated using Eqs. (16).

$$\frac{1}{r_t} = \frac{1}{r_n} + \frac{1}{r_{cs}} \quad (19)$$

where $\frac{1}{r_n}$ is the flexural curvature and $\frac{1}{r_{cs}}$ is the shrinkage curvature. After obtaining the total curvature, the deflection due to the load, creep, and shrinkage can be calculated using Eqs. (17).

$$\delta = KL^2 \frac{1}{r_t} \quad (20)$$

where K is the bending moment, L is the span length, and $\frac{1}{r_t}$ is the total curvature. For a prestressed member, the deflection caused by the initial prestressing force and the subsequent loss of prestressing force can be calculated using Eq.(21) and (22), as described in the previous subsection. Finally, to calculate the long-term deflection, accounting for the applied load, shrinkage, creep, and relaxation of steel (FIB - Federation Internationale du Beton, 2013), Eq.(21) can be used:

$$\delta_{total} = a_1 + \delta_{pi} - \delta \quad (21)$$

Here, a_1 is the deflection due to the prestressing force, δ_{pi} is the deflection due to loss of prestressing force, and δ is the deflection due to load, creep, and shrinkage.

The FIB 2010 model is a more advanced tool than ACI 209R-92 for estimating long-term deflections in prestressed concrete beams. However, it has specific limitations, particularly concerning its complexity, sensitivity to input parameters, and assumptions about material behavior and structural interactions. The model employs a multiplicative approach to combine the effects of creep and shrinkage, which can lead to inaccuracies when these effects interact nonlinearly. This approach is more intricate than the additive method used in simpler models, such as ACI 209R-92. Furthermore, while the FIB 2010 model includes supplementary cementitious materials (SCMs) like fly ash and slag, its predictions may not adequately reflect the distinct characteristics present in high-volume SCM mixtures or ternary blends.

3.3. Long-Term Deflection Calculation According to the Displacement Method

The displacement method for calculating deflection is based on an analytical approach that integrates the principles of structural mechanics and elasticity theory. This method utilizes the principle of equilibrium, transformation of the deflection equation under load, plays a critical role in the formula as it establishes the relationship between the internal forces and the resulting deformations. Stiffness is a key parameter in determining the extent of deflection caused by the applied load. Using these approaches, the deflection formula allows for an accurate estimation of structural deformation. The long-term deflection formula based on the displacement method is as follows:

The first step is to determine the stress and strain at t_0 . The instantaneous axial strain at the center and curvature is expressed in Eqs. (22).

$$\begin{Bmatrix} \mathcal{E}_O(t_0) \\ \Psi(t_0) \end{Bmatrix} = \frac{1}{E(AI-B^2)} \begin{bmatrix} I & -B \\ -B & A \end{bmatrix} \begin{Bmatrix} N \\ M \end{Bmatrix}_{equivalent} \quad (22)$$

where A , B , and I represent the area, first moment, and second moment of the transformed section at time t_0 , respectively; E is the modulus of elasticity of the concrete; N is the axial

normal force; and M is the bending moment. The concrete stresses at the top and bottom fibres are given in Eqs. (23).

$$\sigma_c(t_0) = Ec(t_0)[\mathcal{E}_O(t_0) + \Psi(t_0)y] \quad (23)$$

where $Ec(t_0)$ is the age-adjusted modulus of elasticity of concrete; $\mathcal{E}_O(t_0)$ is the instantaneous axial strain; $\Psi(t_0)$ is the curvature immediately after prestressing, and y is the distance from the reference point O of the layer considered. The next stage is the change in stress and strain owing to creep, shrinkage, and relaxation. The age-adjusted elasticity modulus of concrete is given by Eqs. (24).

$$\bar{E}_c(t, t_0) = \frac{Ec(t_0)}{1 + \chi\varphi} \quad (24)$$

where $Ec(t_0)$ is the modulus of elasticity of the concrete at the initial time t_0 . χ is the aging coefficient of concrete, and φ is the creep coefficient. The stress in the concrete at the top and bottom fibres when the strain due to creep and shrinkage is artificially restrained, is described in Eqs. (2518).

$$\sigma_{restrained} = -\bar{E}_c(t, t_0)[\varphi(t, t_0)\mathcal{E}_c(t_0) + \mathcal{E}_{cs}] \quad (25)$$

where $\bar{E}_c(t, t_0)$ is the age-adjusted elasticity modulus of concrete, $\varphi(t, t_0)$ is the creep coefficient of concrete, $\mathcal{E}_c(t_0)$ is the instantaneous strain, and \mathcal{E}_{cs} is the shrinkage strain. The restraining forces are expressed by Eqs. (26).

$$\begin{Bmatrix} \Delta N \\ \Delta M \end{Bmatrix}_{creep} = - \sum_{i=1}^m \left\{ \bar{E}_c \varphi \begin{bmatrix} A_{ci} & B_{ci} \\ B_{ci} & I_{ci} \end{bmatrix} \begin{Bmatrix} \mathcal{E}_O(t_0) \\ \Psi(t_0) \end{Bmatrix} \right\}_i \quad (26)$$

The subscript i refers to the i^{th} part of the section, and m is the total number of concrete parts. A_{ci} , B_{ci} , and I_{ci} are respectively the area of concrete of the i^{th} part and its first and second moment about an axis through the reference point O. \bar{E}_{ci} and φ are the age-adjusted modulus of elasticity and creep coefficient for concrete in the i^{th} part. $\mathcal{E}_O(t_0)$ and $\Psi(t_0)$ are the instantaneous axial strain and curvature immediately after prestressing. The forces required to prevent shrinkage are given by Eqs. (27).

$$\begin{Bmatrix} \Delta N \\ \Delta M \end{Bmatrix}_{shrinkage} = - \sum_{i=1}^m \left\{ \bar{E}_c \mathcal{E}_{cs} \begin{bmatrix} A_{ci} \\ B_{ci} \end{bmatrix} \right\}_i \quad (27)$$

where \mathcal{E}_{cs} is the free shrinkage for the period t_0 to t , and A_{ci} , B_{ci} are respectively the area of concrete. The forces necessary to prevent strain due to the relaxation of the prestressed steel can be described by Eqs. (28).

$$\begin{Bmatrix} \Delta N \\ \Delta M \end{Bmatrix}_{relaxation} = \sum \left\{ \begin{Bmatrix} A_{ps} \Delta \bar{\sigma}_{pr} \\ A_{ps} y_{ps} \Delta \bar{\sigma}_{pr} \end{Bmatrix} \right\}_i \quad (28)$$

The subscript I in this equation refers to the prestressed steel layer. A_{ps} is its cross-sectional area and y_{ps} is its distance below the reference point O , and $\Delta\bar{\sigma}_{pr}$ is the reduced relaxation during the period from t_0 to t . Then, the change in the axial strain in the center and curvature is given by Eqs. (29).

$$\begin{Bmatrix} \Delta\mathcal{E}_O \\ \Delta\Psi \end{Bmatrix} = \frac{1}{\bar{E}_c(\bar{A}\bar{I} - \bar{B}^2)} \begin{bmatrix} \bar{I} & -\bar{B} \\ -\bar{B} & \bar{A} \end{bmatrix} \begin{Bmatrix} -\Delta N \\ -\Delta M \end{Bmatrix} \quad (29)$$

where \bar{A} , \bar{B} , and \bar{I} are the areas of the age-adjusted transformed section and its first and second moments about an axis through the reference point O . The stress that will develop during the period ($t-t_0$) in concrete, non-prestressed steel, and prestressed steel are given in Eqs. (30), (31), and (32).

$$\Delta\sigma_c = \sigma_{restrained} + \bar{E}c(t, t_0)(\Delta\mathcal{E}_O + y\Delta\Psi) \quad (30)$$

$$\Delta\sigma_{ns} = E_{ns}(\Delta\mathcal{E}_O + y\Delta\Psi) \quad (31)$$

$$\Delta\sigma_{ps} = \Delta\bar{\sigma}_{pr} + \bar{E}_{ps}(\Delta\mathcal{E}_O + y_{ps}\Delta\Psi) \quad (32)$$

where $\sigma_{restrained}$ is the stress in the restrained condition, $\bar{E}c(t, t_0)$ is the age-adjusted modulus of elasticity, $\Delta\mathcal{E}_O$ and $\Delta\Psi$ are the axial strain and curvature, $\Delta\bar{\sigma}_{pr}$ is the reduced relaxation during the period t_0 to t , E_{ns} is the modulus of elasticity of non-prestressed steel, and \bar{E}_{ps} is the modulus of elasticity of prestressed steel. The final stage of the displacement method was used to calculate long-term deflection. The formula for calculating the long-term deflection using the displacement method is shown in Eqs. (33).

$$\delta_1 = \frac{l^2}{96}(\Psi_1 + 10\Psi_2 + \Psi_3) \quad (33)$$

where l is the span length of the prestressed beam and Ψ_1, Ψ_2, Ψ_3 are the total curvature.

The displacement method presents several noteworthy advantages compared to traditional code-based approaches when calculating long-term deflections in prestressed concrete beams. This method is especially beneficial for handling complex geometrical configurations, accommodating nonlinear material behaviors, and incorporating time-dependent phenomena such as creep and shrinkage. Specifically, the displacement method allows for more accurate modeling of how various structural factors—like varying load conditions and support placements—affect deflections over time. However, it is essential to recognize that this technique has challenges. The need for precise assumptions regarding material properties and environmental influences can pose obstacles, especially in scenarios where data is scarce or incomplete. Thus, while the displacement method can enhance the precision of deflection predictions, its implementation demands careful consideration and comprehensive data management to ensure reliable outcomes in its applications.

4. Methods

4.1. The Investigated Prestressed Beam

The sample used in this study was a prestressed beam with a span of 13.05 meter and dimensions of 350 x 700 mm, with a tendon duct consisting of seven strands. This prestressed beam, sourced from a school building, is primarily used as a hall and is supported by two columns. As a result, it can be concluded that the two ends of the beam are clamped, as both ends are cast together with the columns. The specifications of the prestressed concrete materials used in this study are presented in Figure 1 and Table 1.

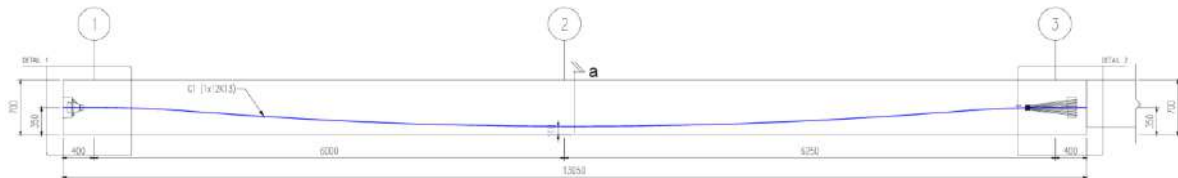


Figure 1. The sample of prestressed beam with span of 13.05 meter with dimensions of 350 x 700 mm.

The longitudinal stirrups were arranged with 2 Φ 19 bars, spaced along the length of the beam at intervals of Φ 13 @200. For the prestressed beams, the prestressed steel strands were positioned at the center of the beam with an eccentricity of 240 mm. The strands used in the prestressed beam were ASTM A416 Grade 720. The material parameters of the three steel-bar types are listed in Table 1.

Table 1. Steel bar diameter and mechanical properties

Steel bar type	Diameter (mm)	Yield strength (MPa)	Elastic modulus
Longitudinal steel bar	19	400	200
Stirrup	13		
Steel strand (prestress)	12.7	1860	195

4.2. Input Parameters

The creep and shrinkage prediction uses two codes: ACI 209R-08 and CEB FIP 1990. These two models have different input parameters (Table 2) for calculating shrinkage and creep. However, both codes share several common parameters, including relative humidity, volume-to-surface ratio, and age of loading. ACI 209R-08 also requires a fine aggregate factor, which can influence shrinkage and creep through various mechanisms, such as resisting volumetric changes and causing excessive water absorption, which in turn alters the mix's elasticity and stiffness. ACI 209R-08 also considers the impact of the air content. Both models consider the cement content, which plays an important role in binding materials that affect shrinkage in concrete.

Table 2. Overview of the input parameters used in various shrinkage and creep prediction models.

Input	ACI 209R-08	CEB-FIP 1990
Age at the start of drying	X	X
Age at the start of loading	X	X
Ambient relative humidity	X	X

Slump factor	X	
Fine aggregate factor	X	
Cement content factor	X	
Air content factor	X	
Initial moist curing coefficient	X	
Volume-to-surface ratio	X	X
Concrete age		X
Cement type		X
Compressive strength		X

The influence of temperature on the long-term deflection of prestressed concrete is well-documented (Aili and Torrenti, 2020). Temperature variations can alter materials' morphology and physical characteristics, thus affecting their shrinkage and creep responses, and subsequently influence the long-term deflection. However, in the context of this study, which aims to compare displacement methods, we have adopted a framework where the temperature is constant throughout the designated study period. This simplification is deemed adequate for comparative analysis, enabling a more concentrated assessment of the primary variable under investigation, devoid of confounding temperature fluctuations. While it is acknowledged that environmental variables can impact the overall outcomes, this methodological choice is justifiable within the study's scope.

4.3. Output Parameters

The problem-solving method for estimating long-term deflection was divided into three phases. The first phase involves identifying the shrinkage and creep that occurs in prestressed concrete and estimating the long-term shrinkage and creep values. A prediction model for shrinkage and creep is developed by correlating factors that affect shrinkage and creep. The methods for developing long-term shrinkage and creep predictions can be accommodated by ACI 209.2R-08. Guide for Modeling and Calculating Shrinkage and Creep in Hardened Concrete, 2008 and CEB-FIP Model Code 1990 for Concrete Structures, 1991. In addition to the shrinkage and creep obtained from these two codes, the relaxation of prestressing steel is also estimated using formulas described in Section 2.3. After the three input parameters have been determined, the study predicts the amount of prestress loss due to shrinkage, creep, and steel relaxation as well as the long-term deflection that occurs in prestressed concrete due to these three parameters (Jindra *et al.*, 2024). This research method overall is illustrated in Figure 2.

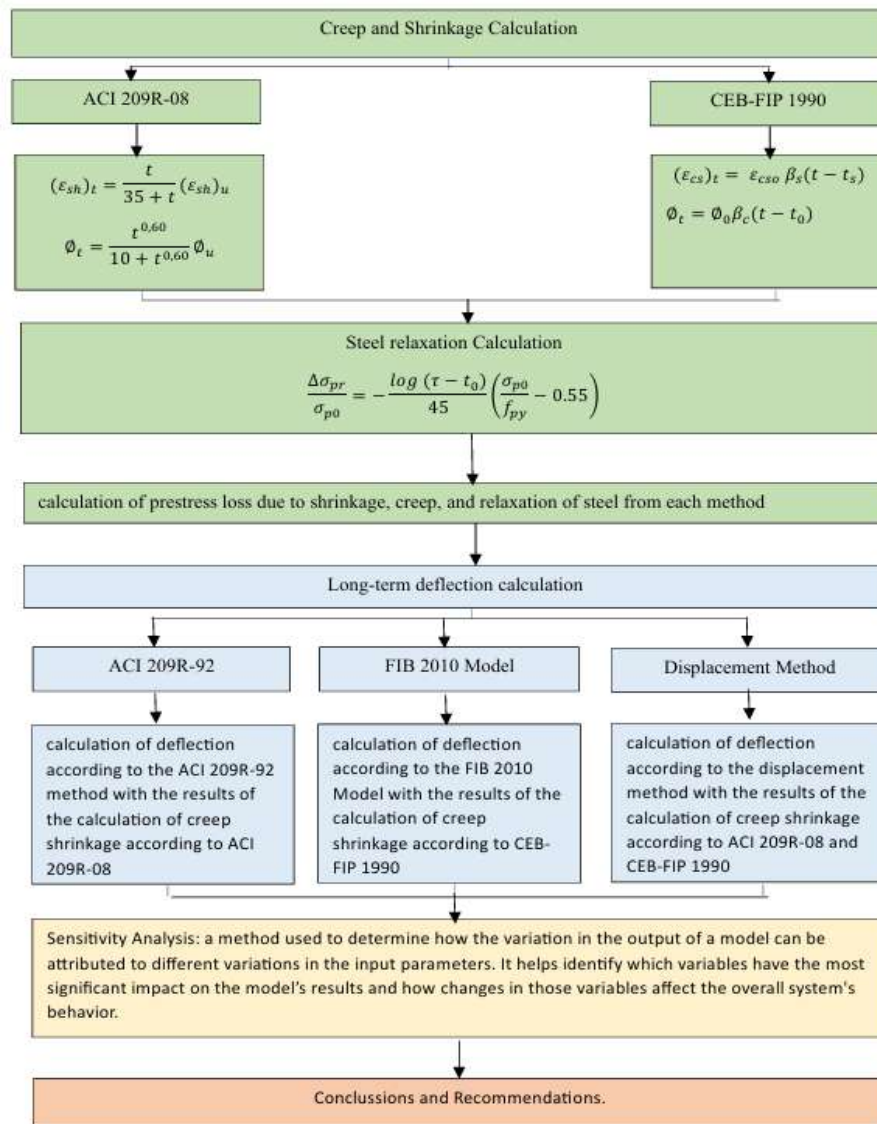


Figure 2. Research method flow chart

Research has demonstrated that both environmental conditions and the material composition of concrete significantly impact its shrinkage behavior. Key environmental variables influencing concrete shrinkage rates include relative humidity, air content, and ambient temperature. Furthermore, the characteristics of the concrete mix, such as the fine aggregate ratio, the volume-to-surface area ratio, and the type of cement utilized, play a critical role in determining the concrete's susceptibility to creep shrinkage. This aligns with the findings of (Shurbert-Hetzel *et al.*, 2023), who underscore the necessity of accounting for these factors in concrete design to enhance the accuracy of shrinkage predictions. Additionally, established design codes, such as those from ACI 209R-08 and CEB-FIP 1990, acknowledge these material and environmental parameters as crucial contributors to shrinkage prediction, given their influence on the concrete's long-term performance. For this reason, the above parameters were included in the sensitivity analysis.

The sensitivity analysis can be conducted using either a statistical or numerical approach. The statistical approach typically employs random sampling from input parameters characterized by specific probability distributions, allowing for the examination of their effects on the output, which is also represented as a distribution. This methodology often employs Monte Carlo Simulation to facilitate the analysis. However, in this study, we lack the requisite data to appropriately define the distribution of the parameters under consideration, rendering the statistical approach infeasible. Consequently, we adopt a numerical or deterministic methodology, wherein small variations are applied to the input parameters, and the resulting changes in output are observed and evaluated

5. Results and Discussions

5.1. Long-term Shrinkage and Creep Prediction

Table 3, Figure 3 and 4 summarize the simplified calculation of creep and shrinkage coefficients of prestressed beam using two codes: ACI 209R-08 and CEB-FIP 1990.

Table 3. Recapitulation of shrinkage and creep coefficient

Time of loading (days)	Shrinkage		Creep	
	ACI 209R-08	CEB-FIP 1990	ACI 209R-08	CEB-FIP 1990
367	-3.89×10^{-4}	-1.88×10^{-4}	0.43	1.67
700	-4.05×10^{-4}	-2.44×10^{-4}	0.43	1.86
900	-4.10×10^{-4}	-2.67×10^{-4}	0.43	1.92
1500	-4.158×10^{-4}	-3.14×10^{-4}	0.42	2.02

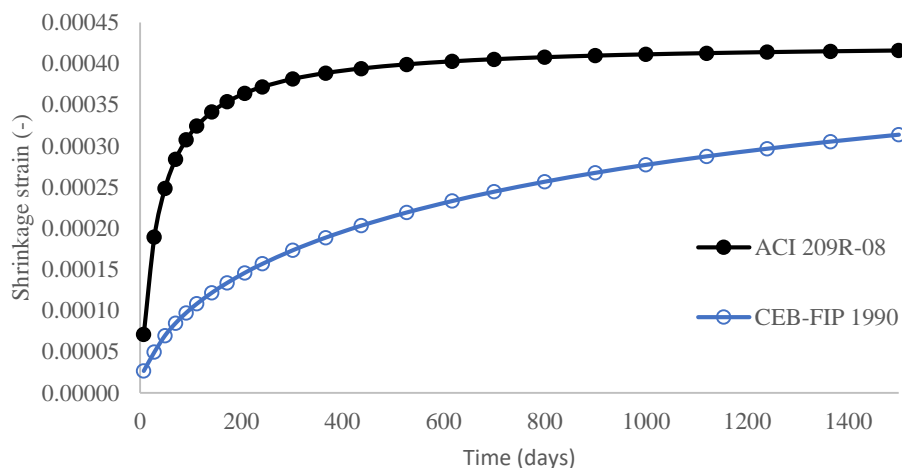


Figure 3. Shrinkage deformation calculation results of prestressed concrete

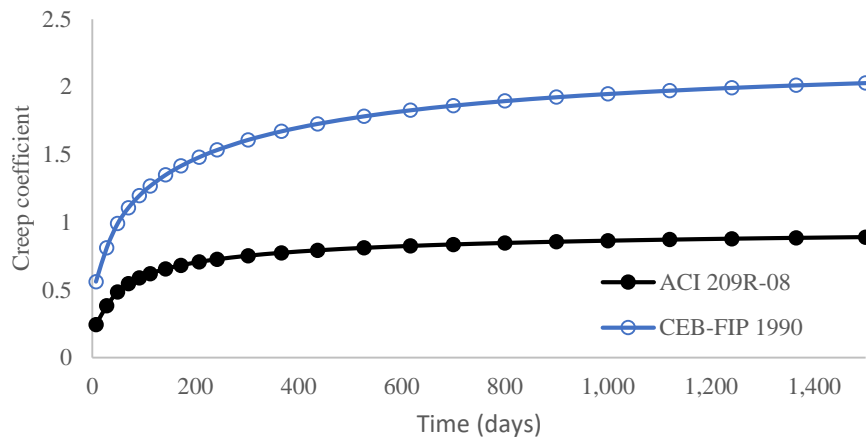


Figure 4. Creep coefficient deformation calculation results of prestressed concrete

As shown in Figure 3, a distinct contrast emerges between the shrinkage predictions of ACI 209R-08 and CEB-FIP 1990. The ACI 209R-08 model demonstrated a sharp increase in shrinkage from the onset of drying, rapidly approaching its maximum value after approximately 300 days. Beyond this point, the change in shrinkage was minimal, suggesting that the material effectively reached a steady state in terms of moisture loss. By contrast, the CEB-FIP 1990 model illustrates a more gradual increase in shrinkage. Despite also showing a rise in shrinkage, this model did so at a diminishing rate; even after a lengthy drying period of 1500 days, the shrinkage continued to rise, albeit very slowly. Moreover, the overall magnitude of shrinkage estimated by the CEB-FIP 1990 model remained lower than that predicted by ACI 209R-08, highlighting significant differences between the approaches of these two models in assessing long-term drying effects. The long-term shrinkage value of CEB-FIP 1990 was approximately 75% of that predicted by ACI 209R-08.

The creep prediction outcomes based on the CEB-FIP 1990 guidelines indicated significantly higher values than those derived from ACI 209R-08 (see Figure 4). Both predictive models exhibited a similar pattern of creep behavior, characterized by a rapid increase in deformation shortly after loading began, ultimately stabilizing at approximately 400 days of loading. However, the magnitude of the creep coefficient estimated by CEB-FIP (1990) was approximately double that of its ACI counterpart. This discrepancy can be attributed to several underlying factors related to the methodologies and assumptions embedded within each code. Specifically, the CEB-FIP 1990 employs a more sophisticated and empirical modelling approach that incorporates a range of variables such as the age of the concrete, its compressive strength, and prevailing environmental conditions. This comprehensive framework tends to yield more conservative estimates, resulting in higher predicted creep values compared with ACI 209R-08, which adopts a more straightforward and simplified model (Fanourakis and Ballim, 2006).

5.2. Prestress Loss Prediction Due to Shrinkage, Creep and Relaxation

The prestress loss in prestressed concrete is the reduces the prestressing force acting on the tendon or prestressing cable (tendon) during the loading process. This study predicted the

time-dependent prestress loss resulting from shrinkage, creep, and steel relaxation (Huang *et al.*, 2025).

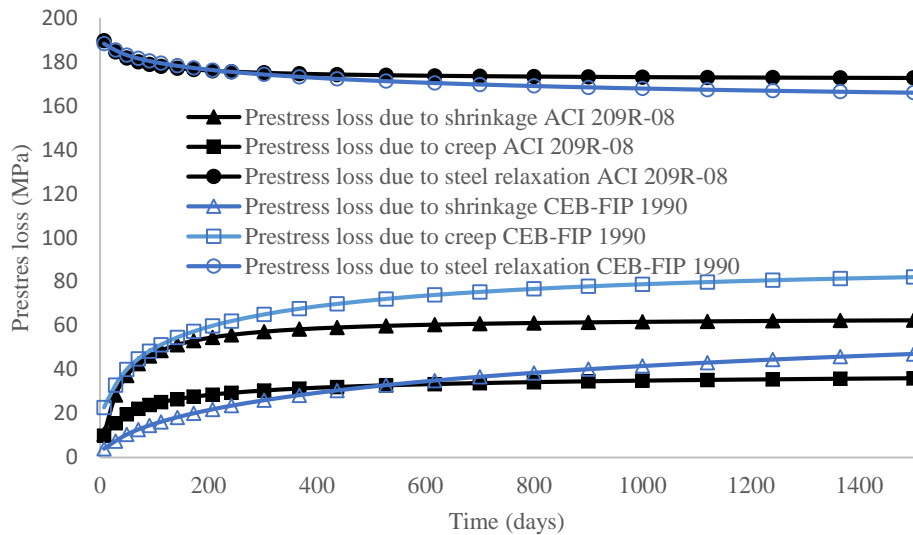


Figure 5. Prestress loss calculation results due to shrinkage, creep, and steel relaxation of prestressed concrete

The analysis of prestress loss, conducted using the CEB-FIP 1990 guidelines, revealed that the losses of prestressing force owing to shrinkage and steel relaxation were consistently lower than those predicted by the ACI 209R-08 model. Conversely, when assessing the prestress loss due to creep, the CEB-FIP 1990 approach produced higher values compared to the ACI 209R-08 counterpart. It is important to note that over time, the total prestress loss resulting from shrinkage, creep, and steel relaxation gradually decreases until it stabilizes at constant values. Notably, the prestress loss attributed to steel relaxation includes both elastic shortening and losses due to shrinkage and creep, suggesting that the total steel relaxation loss exceeds the combined losses from shrinkage and creep. The overall magnitude of these losses, relative to the original prestressing force, was found to be within 17% for the ACI-209R-08 methods and 21% for the CEB-FIP 1990 method. According to the ACI 209R-08 model, the percentages of prestress loss attributed to shrinkage, creep, and steel relaxation were 3%, 1%, and 13%, respectively. The CEB-FIP 1990 model indicates corresponding losses of 3%, 6%, and 12%, respectively.

The assertion that prestress loss attributed to creep and shrinkage is consistently lower than that caused by steel relaxation cannot be universally applied across all types of prestressed concrete beams. This relationship is contingent upon various factors, including the specific concrete mix, the characteristics of the prestressing steel, and prevailing environmental conditions such as humidity and temperature. Consequently, while certain combinations of materials and conditions may yield a scenario where prestress loss from creep and shrinkage is negligible compared to steel relaxation, other scenarios may reveal a more pronounced impact from creep and shrinkage. For instance, in cases involving high-strength concrete or prestressing steel characterized by substantial relaxation properties, the losses due to steel relaxation can overshadow those from creep or shrinkage. Conversely, in concrete formulations

with differing characteristics or with prestressing steel that exhibits a lower relaxation rate, the losses caused by creep and shrinkage may become more significant. Numerous studies have explored this dynamic, comparing the prestress losses due to shrinkage and creep against those resulting from steel relaxation, providing critical insights into the behavior of various prestressed concrete systems (Tadros et al., 1985; Boukendakdji et al., 2017; Han et al., 2023b)

5.3. Long-term Deflection Prediction

Long-term deflection calculations are critical in structural engineering, particularly when assessing the performance of concrete structures over time. Engineers often rely on established code-based methods for these calculations, with two widely recognized references being the ACI 209R-92 and the FIB 2010 Model codes. These codes provide guidelines that account for the time-dependent behavior of concrete, which is essential for accurately predicting deflections due to factors such as shrinkage, creep, and the relaxation of reinforcing steel. The underlying assumption of these code-based methods is that the material behaves elastically and homogeneously throughout its lifetime. This implies that the material properties are treated as consistent and uniform, which simplifies the complex real-world behavior of concrete and steel under loading. The rationale for utilizing code-based deflection calculations lies in their ability to simplify intricate structural models. By reducing complex interactions and behaviors into manageable computations, these codes enable engineers to conduct efficient and effective analyses, ensuring that structures meet safety and performance criteria over their intended lifespan. However, it is important to approach the deflection estimates provided by code-based methods with caution to ensure that they offer accurate safety assessment for structural applications. In this context, Table 4 and Figure 6 present an overview of the long-term deflection characteristics of prestressed beams, as derived from both the simplification method, which is representative of code-based approaches, and the displacement method referenced in (Ghali *et al.*, 2006). The shrinkage, creep, and steel relaxation data for the calculations are based on ACI 209R-08 and CEP-FIP 1990, as outlined in subsections 5.1-5.3. Based on these three parameters, the long-term deflection was estimated using code-based methods (ACI 209R-92 and FIB 2010 model) and the corresponding displacement method.

Table 4. Recapitulation of long-term deflection

Duration of loading (days)	Deflection (mm)			
	Creep and Shrinkage based on ACI 209R-08		Creep and Shrinkage based on CEB-FIP 1990	
	ACI 209R-92	Displacement Method*	Fib 2010 Model	Displacement Method**
367	-8.233	-8.591	-7.390	-7.649
700	-8.506	-8.692	-7.982	-8.281
900	-8.580	-8.726	-8.184	-8.285

1500

-8.693

-8.787

-8.536

-8.300

*Deflection by displacement method using shrinkage and creep based on ACI 209R-08

**Deflection by displacement method using shrinkage and creep based on CEB-FIP 1990

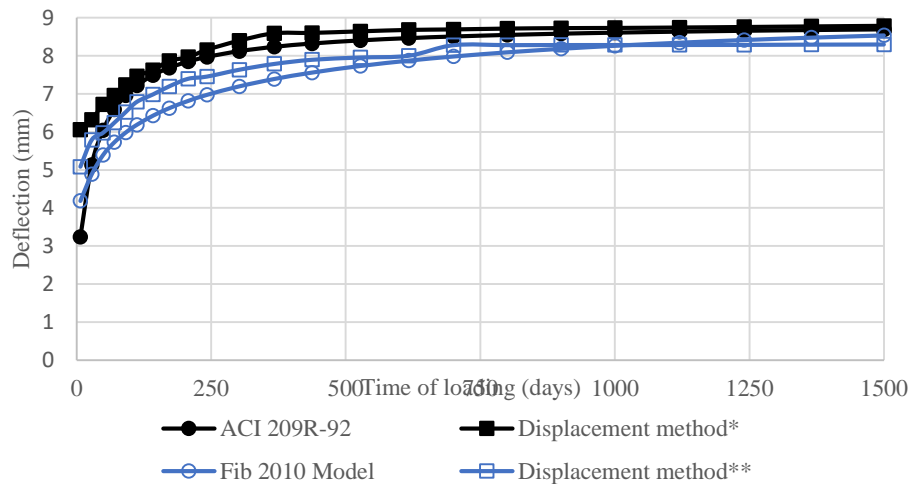
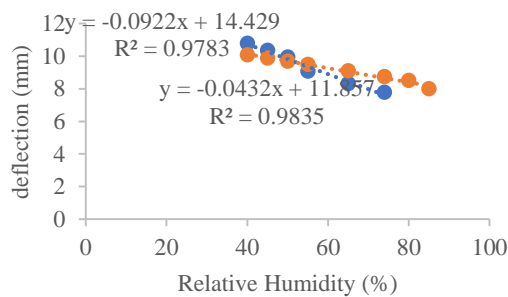


Figure 6. Long-term deflection calculation results with two methods of prestressed concrete

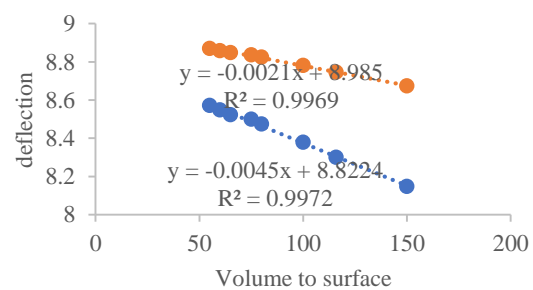
Upon reviewing the data in Table 4 alongside the visual representation in Figure 6, it is evident that the calculations for shrinkage, creep, and relaxation, as outlined in ACI 209R-08 and CEB-FIP 1990 codes, produce comparable values for the long-term deflection of prestressed concrete beams, although the code-based method by ACI 209R-92 gives a slightly higher value. A comparison of the code-based methods with the displacement method revealed that the displacement method consistently showed larger long-term deflections than the code-based calculations. This difference suggests that the code-based methods may not be adequately conservative in their deflection estimations. However, it is worth noting that the observed difference between the two methods remains relatively small, typically within a margin of just 4%. A 4% variance in structural deflection calculations can have significant implications, depending on specific design parameters and prescribed tolerances. For instance, if the code dictates a maximum allowable deflection of $L/360$, which equates to approximately 36.25 mm, a 4% deviation would amount to about 1.45 mm. In many projects, such a degree of deviation may be acceptable. However, this seemingly minor deviation may raise serious concerns in circumstances where tolerances are strict or structural integrity is critical. Therefore, while a 4% variation might not require adjustments to design guidelines, designers should remain cautious, particularly when strict deflection limits are enforced on a project. These findings highlight the need for engineers to reconcile these two approaches when designing prestressed concrete structures, striving for a balance between code compliance and an accurate reflection of long-term deflection behavior.

5.4. Sensitivity Analysis

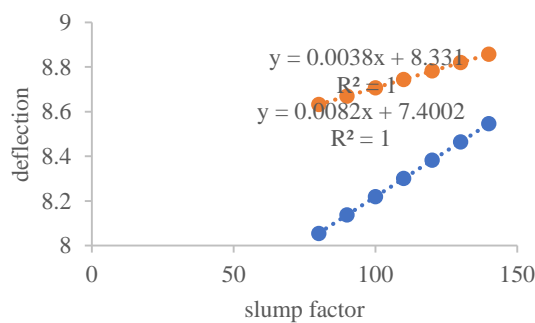
The results obtained from the long-term deflection studies provide a comprehensive analysis of the sensitivity of deflection with respect to various parameters that influence shrinkage, creep, and relaxation behavior of prestressed steel. To conduct a thorough sensitivity analysis, the parameters that significantly affected the shrinkage and creep characteristics of the prestressed beams were systematically varied. In this analysis, we focused on a range of relative humidity levels, specifically from 40% to 85%, as this parameter plays a crucial role in the drying of concrete. Additionally, we examined the influence of the volume-to-surface ratio, which was adjusted from 35 mm to 150 mm, on the rate of moisture loss from the concrete. The slump factor was also varied within the range of 80 – 140 mm to study its effect on the workability and compaction of the mixture. Furthermore, we explored the fine aggregate factor, which ranged from 35% to 60%, recognizing its significance in determining the overall properties of the concrete mix. The cement content was analyzed in the range of 300 to 413 kg/m³, reflecting different mix designs. To account for the presence of air in the mixture, air content levels ranging from 3% to 7% were considered. Moreover, the initial moist-curing duration was set between 7 and 28 days, which is critical for ensuring adequate strength and durability of the concrete. Finally, we examined the compressive of the strength of the concrete, varying from 31.9 to 48 MPa, as it directly correlates with the performance of the material under stress (Shurbert-Hetzel *et al.*, 2023). Based on these considerations, the results highlight the impact of the aforementioned parameters on deflection, as illustrated in Figures 7 and 8. They provide a clear visual representation of how variations in these influential factors can lead to significant changes in the deflection behavior of prestressed beams.



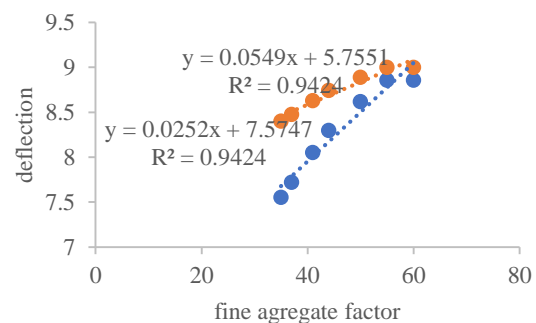
(a) Effect of relative humidity on deflection



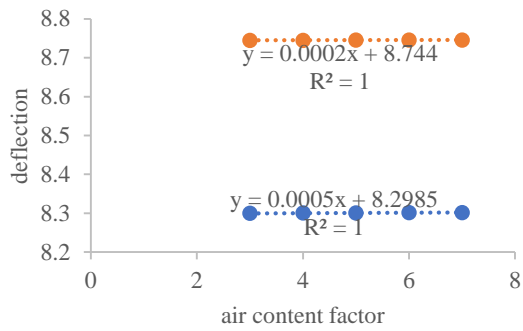
(b) Effect of volume-to-surface ratio on deflection



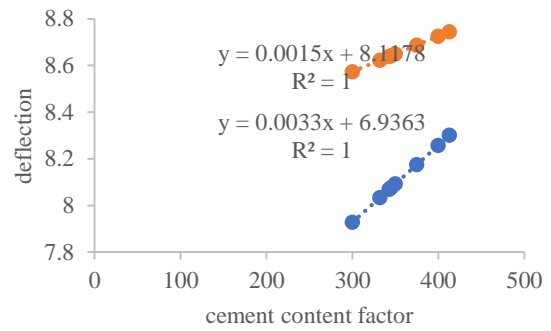
(c) Effect of slump factor on deflection



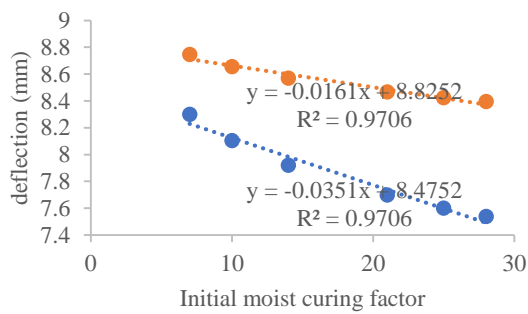
(d) Effect of fine aggregate factor on deflection



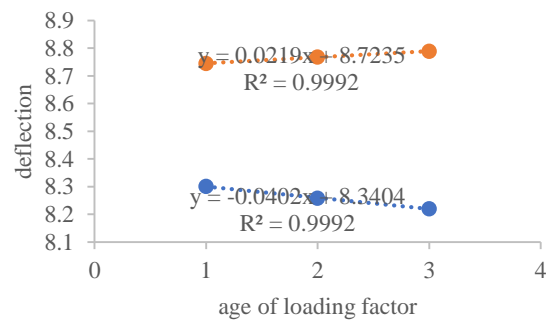
(e) Effect of air content factor on deflection



(f) Effect of cement content factor on deflection



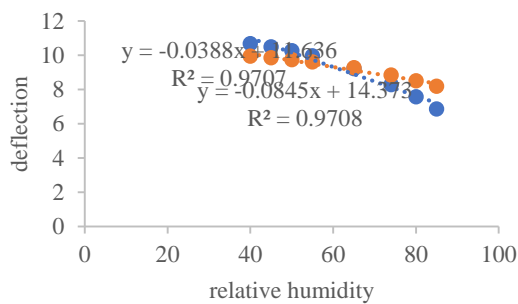
(g) Effect of initial moist curing factor on deflection



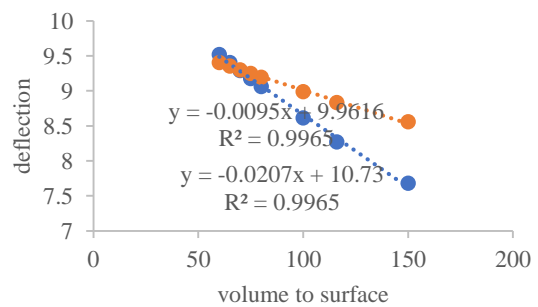
(h) Effect of age of loading factor on deflection

- Deflection by ACI 209R-92 model
- Deflection by displacement method*

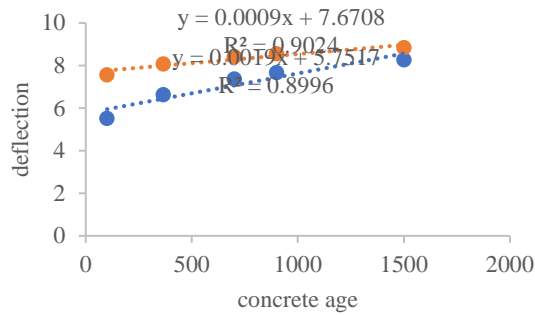
Figure 7(a-g). Sensitivity analysis of deflection parameters according to ACI 209R-08



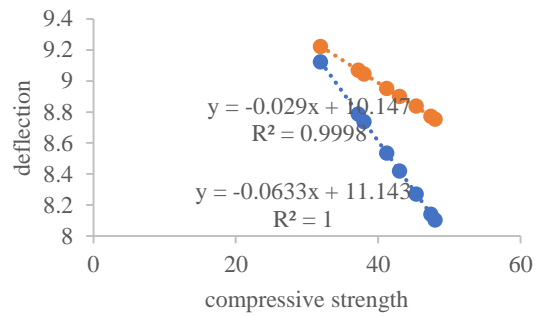
(a) Effect of relative humidity on deflection



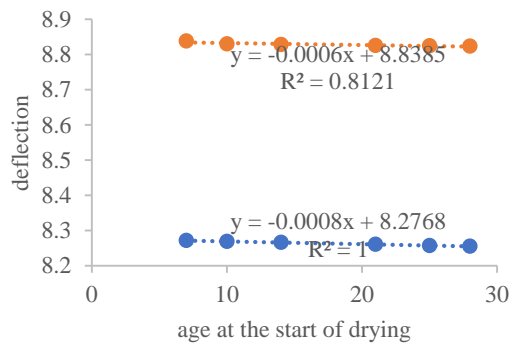
(b) Effect of volume-to-surface ratio on deflection



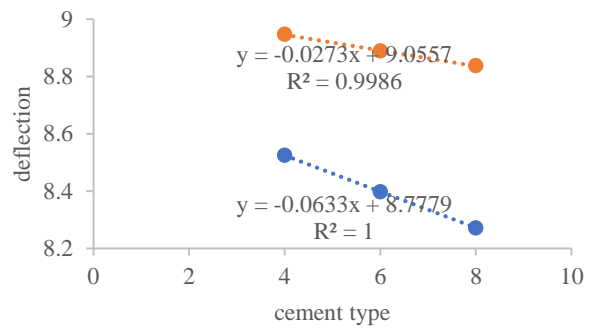
(c) Effect of concrete age of loading on deflection



(d) Effect of compressive strength on deflection



(e) Effect of age at the start of drying on deflection



(f) Effect of cement type factor on deflection

- Deflection with CEB-FIP 1990 method
- Deflection with displacement method

Figure 8(a-f). Sensitivity analysis of deflection parameters according to CEB-FIP 1990

An examination of the multiple parameters influencing the phenomena of creep and shrinkage indicates that not all these factors have a significant impact the deflection of prestressed beams. Among these parameters, relative humidity is the most critical factor affecting the extent of deflection changes. This conclusion is supported by both code-based and displacement methodologies. In particular, the analysis reveals that code-based methods yield a higher percentage of change in deflection when relative humidity varies, compared to the displacement method. This suggests that the former is more sensitive to fluctuations in environmental conditions. Furthermore, the data illustrates a clear relationship; as relative humidity increases, the amount of deflection in the prestressed beam tends to decrease. This trend is visually represented in Figures 9 and 10, which demonstrate the significant influence of humidity levels on deflection, in contrast to the other parameters. Moreover, a comparative analysis of the parameters influencing deflection revealed that both the code-based and displacement methods yielded similar values regarding their effects on deflection. This consistency implies that either approach can be reliably employed to analyze the deflection characteristics of the structure, ensuring that the results are dependable and aligned across different analytical frameworks. Thus, engineers and designers can confidently use either method, knowing that they will obtain comparable insights into the deflection behavior of prestressed beams under varying conditions.

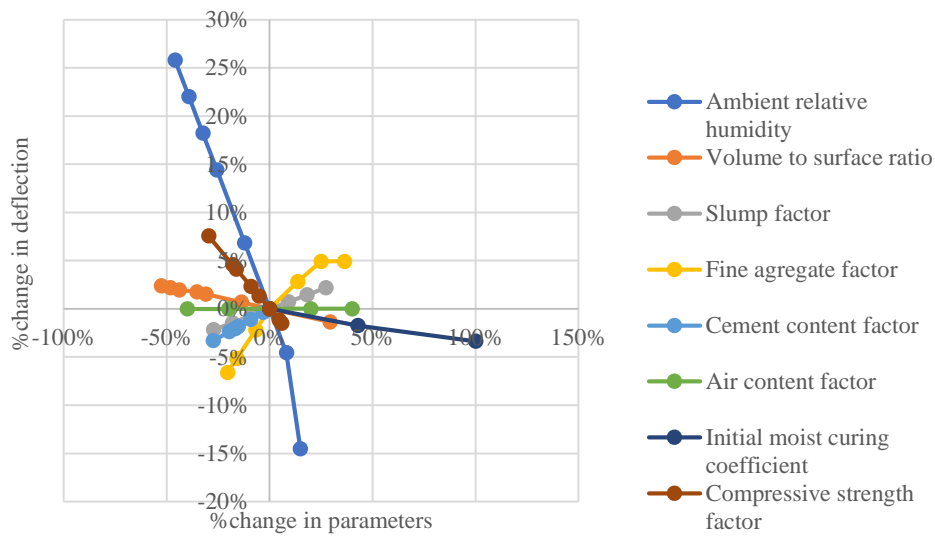


Figure 9 Sensitivity Analysis by Code Based Method

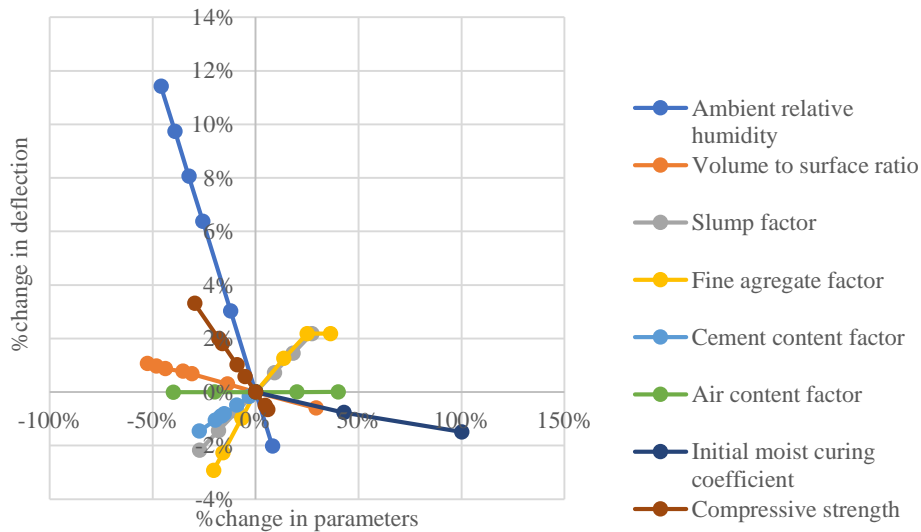


Figure 10. Sensitivity Analysis by Displacement Method

6. Conclusions

The long-term deflection of prestressed concrete beam is influenced by shrinkage, creep, and relaxation.

Based on this prediction, the following conclusions were drawn:

- ACI 209R-08 gives a faster rate of shrinkage and consistently higher magnitude of shrinkage than the CEB-FIP 1990. On the other hand, the CEB-FIP 1990 estimates a creep coefficient of about twice that predicted by ACI 209R-08.
- The losses of prestressing force due to creep and shrinkage are minor compared to the steel relaxation. The total losses of prestressing force are within a range of 17-21%, where the calculated losses based on ACI 209R-08 data are lower than the CEB-FIP 1990. The loss of

prestress within this range represents the average prestress reduction that designers should anticipate for typical prestressed beam structures.

- The deflection estimated by the Fib 2010 Model is initially smaller than the deflection by ACI 209R-92. However, as time increases, the two deflections approach similar values. Both code-based methods give a lower estimation (within 4%) of deflection compared to the displacement method. This seemingly minor deviation could pose significant risks in scenarios where tolerances are tightly controlled or the integrity of the structure is paramount.
- The most significant parameter affecting the deflection according to ACI 209R-92 and Fib 2010 Model is relative humidity. This finding confirms the critical role of environmental conditions in the long-term behavior of prestressed concrete beams. Engineers must carefully consider local relative humidity during design, material selection, and construction to ensure that deflections remain within acceptable limits and that the structure performs satisfactorily over its service life.
- This research employed a typical prestressed concrete beam to evaluate the efficacy of the code-based method in comparison to the displacement method for estimating deflection. Future studies should encompass a wider array of project scenarios, diverse loading histories, and various environmental conditions. Such investigations can offer a more nuanced analysis of the benefits and drawbacks of each method for estimating long-term deflection, thereby assisting in selecting the most appropriate method in various real-world situations.

References

- ACI 209.2R-08. (2008), *Guide for Modeling and Calculating Shrinkage and Creep in Hardened Concrete*, American Concrete Institute. USA, <http://www.civil.northwestern.edu/people/bazant/PDFs/Papers/R21.pdf>.
- ACI 209R-92. (1997), *Prediction of Creep, Shrinkage, and Temperature Effects in Concrete Structures*, American Concrete Institute. USA, http://civilwares.free.fr/ACI/MCP04/209r_92.pdf.
- Aili, A. and Torrenti, J.M. (2020), “Modeling long-term delayed strains of prestressed concrete with real temperature and relative humidity history”, *Journal of Advanced Concrete Technology*, Japan Concrete Institute, Vol. 18 No. 7, pp. 396–408, <https://doi.org/10.3151/jact.18.396>.
- Bello, B.R., Dela Cruz, O.G., Muhi, M.M. and Guades, E.J. (2024), “Enhancing the Flexural Capacity of Reinforced Concrete Beam by Using Modified Shear Reinforcement”, *Civil Engineering Journal (Iran)*, Vol. 10 No. 6, pp. 1720–1741, <https://doi.org/10.28991/CEJ-2024-010-06-02>.
- Boukendakdji, M., Touahmia, M. and Achour, M. (2017), “Comparative Study of Prestress Losses”, *Engineering, Technology & Applied Science Research*, Vol. 7, pp. 1633–1637, <https://doi.org/10.48084/etasr.1172>.
- Comite Euro-International Du Beton. (1993), *CEB-FIP Model Code 1990: Design Code*, London: T. Telford, 1993., <https://doi.org/10.1680/ceb-fipmc1990.35430>.

- Cui, J. and Wu, P. (2024), "Analysis and Optimization Algorithm of Creep Sensitivity for Concrete Section during Shrinkage", PREPRINT (Version 1) available at *Research Square*, <https://doi.org/10.21203/rs.3.rs-4499478/v1>.
- El-Azab, A. and Mohamed, H.M. (2014), "Effect of tension lap splice on the behavior of high strength concrete (HSC) beams", *HBRC Journal*, Vol. 10 No. 3, pp. 287–297, <https://doi.org/10.1016/j.hbrcj.2014.01.002>.
- Fang, Y., Mao, J., Zhang, Y., Jin, W., Tang, D. and Zhang, J. (2021), "Calculation of Deflection and Stress of Assembled Concrete Composite Beams under Shrinkage and Creep and Its Application in Member Design Optimization", *KSCE Journal of Civil Engineering*, Vol. 25 No. 9, pp. 3458–3476, <https://doi.org/10.1007/s12205-021-2092-4>.
- Fanourakis, G. and Ballim, Y. (2006), "An assessment of the accuracy of nine design models for predicting creep in concrete", *Journal of the South African Institution of Civil Engineering*, Vol. 48 No. 4, pp. 2–8, <https://doi.org/10.10520/EJC26992>.
- FIB - Federation Internationale du Beton. (2013), *Model Code for Concrete Structures 2010*, Ernst & Sohn, <https://doi.org/10.1002/9783433604090>.
- Ghali, A., Favre, R. and Elbadry, M. (2006), *Concrete Structures: Stresses and Deformations, Third Edition.*, Taylor & Francis Group, London and New York.
- Ghoniem, A.G., Gamal, M. and Aboul Nour, L. (2024), "Lightweight Fiberglass Concrete Beams of Varying Steel Reinforcement and Shear-Span Depth Ratios", *Civil Engineering Infrastructures Journal*, p. , <https://doi.org/10.22059/ceij.2024.372257.2010>.
- Gilbert, R.I. (2001), "Shrinkage, Cracking and Deflection-the Serviceability of Concrete Structures", *Electronic Journal of Structural Engineering*, Vol. 1, pp. 15–37, <https://doi.org/10.56748/ejse.1121>.
- Han, W., Tian, P., Lv, Y., Zou, C. and Liu, T. (2023a), "Long-Term Prestress Loss Calculation Considering the Interaction of Concrete Shrinkage, Concrete Creep, and Stress Relaxation", *Materials*, Vol. 16 No. 6, <https://doi.org/10.3390/ma16062452>.
- Han, W., Tian, P., Lv, Y., Zou, C. and Liu, T. (2023b), "Long-Term Prestress Loss Calculation Considering the Interaction of Concrete Shrinkage, Concrete Creep, and Stress Relaxation", *Materials*, Vol. 16 No. 6, <https://doi.org/10.3390/ma16062452>.
- Huang, Z., Cao, J., Yang, Y., Gong, F., Zeng, B., Zhao, Y. and Maekawa, K. (2025), "Long-term deformation and prestress loss of PRC beam under vari-humidity environment: Preliminary experiments and multi-scale simulations", *Engineering Structures*, Vol. 322, <https://doi.org/10.1016/j.engstruct.2024.119122>.
- Jindra, D., Hradil, P. and Kala, J. (2024), "Stress relaxation of concrete beams caused by creep and shrinkage effects", edited by Drusa, M., Kadela, M., Rybak, J., Segalini, A. and Krušínský, P. *MATEC Web of Conferences*, Vol. 396, p. 05018, <https://doi.org/10.1051/mateconf/202439605018>.
- Kristiawan, S.A. and Nugroho, A.P. (2017), "Creep Behaviour of Self-compacting Concrete Incorporating High Volume Fly Ash and its Effect on the Long-term Deflection of Reinforced

- Concrete Beam”, *Procedia Engineering*, Vol. 171, pp. 715–724, <https://doi.org/10.1016/j.proeng.2017.01.416>.
- Peng, C., Liu, Z., Xue, J., Chen, Z. and Ren, B. (2025), “Calculation method of deflection of high strength steel reinforced ultra-high-performance concrete beam”, *Structures*, Vol. 71 No. October 2024, p. 108026, <https://doi.org/10.1016/j.istruc.2024.108026>.
- Reybrouck, N., Van Mullem, T., Taerwe, L. and Caspeele, R. (2020), “Influence of long-term creep on prestressed concrete beams in relation to deformations and structural resistance: Experiments and modeling”, *Structural Concrete*, Vol. 21 No. 4, pp. 1458–1474, <https://doi.org/10.1002/suco.201900418>.
- Shurbert-Hetzel, C., Daneshvar, D., Robisson, A. and Shafei, B. (2023), “Data-enabled comparison of six prediction models for concrete shrinkage and creep”, *Case Studies in Construction Materials*, Vol. 19, <https://doi.org/10.1016/j.cscm.2023.e02406>.
- Tadros, M.K., Ghali, A. and Meyer, A.W. (1985), “Prestressed Loss and Deflection of Precast Concrete Members”, *PCI Journal*, No. Januari-February, pp. 114–141. <https://doi.org/10.15554/pcij.01011985.114.141>
- Teng, L., Zhang, R. and Khayat, K.H. (2022), “Tension-Stiffening Effect Consideration for Modeling Deflection of Cracked Reinforced UHPC Beams”, *Sustainability (Switzerland)*, Vol. 14 No. 1, <https://doi.org/10.3390/su14010415>.
- Yang, M., Jin, S. and Gong, J. (2020), “Concrete Creep Analysis Method Based on a Long-Term Test of Prestressed Concrete Beam”, *Advances in Civil Engineering*, Vol. 2020, <https://doi.org/10.1155/2020/3825403>.
- Zhang, H., Guo, Q.Q. and Xu, L.Y. (2023), “Prediction of long-term prestress loss for prestressed concrete cylinder structures using machine learning”, *Engineering Structures*, Vol. 279, <https://doi.org/10.1016/j.engstruct.2022.115577>.
- Zhang, S. and Hamed, E. (2020), “Application of various creep analysis methods for estimating the time-dependent behavior of cracked concrete beams”, *Structures*, Vol. 25, pp. 127–137, <https://doi.org/10.1016/j.istruc.2020.02.029>.
- Zhou, Y., Chen, W. and Yan, P. (2022), “Measurement and modeling of creep property of high-strength concrete considering stress relaxation effect”, *Journal of Building Engineering*, Vol. 56, p. 104726, <https://doi.org/10.1016/j.jobbe.2022.104726>.
- Zhu, L., Wang, J.-J., Li, X., Zhao, G.-Y. and Huo, X.-J. (2020), “Experimental and numerical study on creep and shrinkage effects of ultra high-performance concrete beam”, *Composites Part B: Engineering*, Vol. 184, p. 107713, <https://doi.org/10.1016/j.compositesb.2019.107713>.